Numerical study on coalescence behavior of suspended drop pair in viscous liquid under uniform electric field

Cite as: AIP Advances **8**, 085215 (2018); https://doi.org/10.1063/1.5045747
Submitted: 23 June 2018 . Accepted: 13 August 2018 . Published Online: 21 August 2018

Zhentao Wang, Kai Dong, Lin Tian, Junfeng Wang, and Jiyuan Tu

Numerical study on coalescence behavior of suspended drop pair in viscous liquid under uniform electric field

Zhentao Wang,[1,a] Kai Dong,[1] Lin Tian,[2] Junfeng Wang,[1] and Jiyuan Tu[2,a]
[1]*School of Energy and Power Engineering, Jiangsu University, Zhenjiang 212013, China*
[2]*School of Mechanical and Automotive Engineering, RMIT University, Bundoora 3083, Australia*

(Received 23 June 2018; accepted 13 August 2018; published online 21 August 2018)

Coalescence of drops under externally applied electric field is a significant physical process, which has been applied in many applications such as emulsion breakup, electric dehydration and raindrop formation. The morphological characteristics of two identical adjacent drops under uniform electrical strength were numerically investigated in present study. From the simulated morphologies, the behavior of the meniscus, the major axis, the minor axis, and the cone angle of coalesced drop were analyzed in details. The results indicated that drop coalescence was dependent on the electric field strength, and only below a critical threshold, coalesce occurred. Though variation might occur in lengths of the meniscus, major\minor axis, and size in cone angles, a steady state can always be reached under which electro-coalescence complete. On the other hand, drops failed to coalesce if they could not reach a steady state, and even the coalesced drop rupture due to oversized electric filed strength. Analysis of coalescence behavior of suspended drop pair in viscous liquid under uniform electric field could further promote our understanding on the physical phenomenon of electro-coalescence and provide insight for the design of the electro-coalescers in practical applications. https://doi.org/10.1063/1.5045747

I. INTRODUCTION

Dispersed drops in viscous liquid may experience complex evolution such as movement, deformation, breakage, coalescence and recoil depending on the electric field strength and fluid properties subject to an externally applied field.[1–3] This phenomenon is widely present in liquid/liquid processes of many industrial applications such as emulsion breaking, inkjet printing, coalescence and biochemical processes. In petroleum industry, electrical demulsification is frequently utilized to remove water drops from crude oil. In electro-coalescence, adjacent drops approach, contact, and finally coalesce into a larger drop due to Colombian attraction in an external electric field.[4,5] It is shown that the presence of an electric field promotes contact between drops, and greatly improves drops coalescence efficiency. Therefore, electro-coalescence is considered as an important method and technology to enhance oil-water separation in petroleum industry.

In the past few decades, experimental and numerical studies have been carried out extensively to better understand the process and dynamics of drop-drop electro-coalescence subject to an external electric field. The electro-coalescence process typically contains three stages including drops approaching to each other, film thinning/drainage, and film rupture leading to drop coalescence.[5–7] Other possible mechanisms such as drop chain formation,[8,9] dipole-dipole coalescence,[10] electrophoresis,[11] dielectrophoresis,[12] and random collisions[13] were also mentioned or discussed. Taylor[9] proposed a two-step mechanism of chain formation and coalescence for water-in-oil dispersion as a result of potential difference between adjacent drops due to induced charges. Two adjacent

[a]Email: Author to whom correspondence should be addressed. wickol@hotmail.com and Jiyuan.tu@rmit.edu.au

spherical drops could produce dipole-dipole coalescence as a result of the classical interactions of the electrostatic forces between them.[13] In electro-coalescence, charged drops may enact a body force on the dispersed drops, originated as electrophoretic forces from polarized drops in divergent fields.[14] Four possible scenarios involving drop contacting, surface instability, interfacial layer electrostriction, and shockwave from electric breakdown were also reported.[11] In the process of electro-coalescence, several mechanisms may be involved, while the dominant mechanism could depend on the electric field type, electrode geometry, dispersed phase volumetric fraction, the liquid type, and other operating parameters.

Typical parameters of interests in electro-coalescence process are electric field (DC or AC) type,[15–23] applied frequency,[23,24] electrode geometry,[25] average initial drop size, liquid properties,[26–30] hold-up fraction of the dispersed phase.[31–33] Although it is well known that high electric field could assist coalescence, details on the various factors affecting the coalescence process are not yet fully understood so far. A number of numerical studies have been performed to investigate the electro-coalescence of liquid drops by using direct numerical simulation,[34] VOF (volume-of-fluid) method,[35–37] Lattice Boltzmann simulations,[38,39] smoothed particle hydrodynamics,[40] and molecular dynamics simulations.[41] These studies provided significant information to analyze the dynamic behavior of drop-drop electro-coalescence. Choi et al[42] numerically investigated the coalescence of two compressed drops adjacent to each other, and provided detailed morphological characteristics when viewing the drops from minor axis, major axis, and the meniscus liquid bridge. Despite of well-done prior studies, more work is needed to understand the morphological characteristics of coalesced drops to the physical process.

In the present paper, electro-coalescence of two identical adjacent drops was numerically studied and examined by solving Navier-Stokes equation where the interface was tracked by VOF (volume-of-fluid) method. At the same time, surface charge of the drops was simulated using leaky dielectric theory. Prior to the investigation, single drop deformation was carried out for model validation. Morphological characteristics of the two adjacent drops were recorded and detailed evolution of the electro-coalescence process from perspectives of the minor axis, major axis and meniscus liquid bridge were discussed subject to typical electric field strength. The present study could help better understand the electro-coalescence phenomena in an externally applied electric field.

II. MATHEMATICAL MODEL AND BOUNDARY CONDITIONS

A. Assumptions

For dispersed drops initially suspended in an immiscible viscous liquid, the governing equations of coalescence are established under the following assumptions. The two different immiscible liquids are homogeneous Newtonian and incompressible. The flow is laminar and axisymmetric. The thermal effect is usually neglected. The two dispersed drops are identical. The gravity is neglected because the densities of the two fluids are almost same. Two-dimensional flow model is applicable.[1,2,43]

Governing equations for two-phase flow

For the incompressible flow, continuity equation is described as:

$$\nabla \cdot \mathbf{u} = 0 \tag{1}$$

where $\mathbf{u}$ is the velocity of fluid.

The Navier-Stokes equation of the two-phase flow should include the interface tension and electric stress and given as:

$$\rho\left(\frac{\partial \mathbf{u}}{\partial t} + \mathbf{u} \cdot \nabla \mathbf{u}\right) = -\nabla p + \nabla \cdot \boldsymbol{\tau} + \mathbf{F}_S + \mathbf{F}_e \tag{2}$$

where ρ is the density, p is the pressure, μ is the dynamic viscosity of fluid. $\mathbf{F}_s$ is the body force due to surface tension, while $\mathbf{F}_e$ is the body force due to electric field. Moreover, $\boldsymbol{\tau}$ the strain rate tensor given by

$$\boldsymbol{\tau} = \mu\left[\nabla \mathbf{u} + (\nabla \mathbf{u})^T\right] \tag{3}$$

In Eq. (2), source of the surface tension ($\mathbf{F}_s$) is present only in domain infinitesimal close to the interface. The interface is confirmed by the phase volume faction (α) with $0 < \alpha_i < 1$. The $\mathbf{F}_s$ is considered as a body force, and not a surface force applied to the boundary. CSF (continuum surface tension) method is used to calculate the surface tension force at interface as in the following,[44]

$$\mathbf{F}_s = \gamma \frac{\rho\kappa\nabla\alpha}{\frac{1}{2}(\rho_i + \rho_o)} \tag{4}$$

where $\boldsymbol{\gamma}$ is the surface tension coefficient, $\nabla\alpha$ is the gradient of volume fraction of the phase which is the surface normal in this work,

$$\mathbf{n} = \nabla\alpha_i \tag{5}$$

κ is the curvature defined as

$$\kappa = \nabla \cdot \mathbf{n} \tag{6}$$

ρ_i is the droplet density, ρ_o is the outer liquid density,

$$\rho = \alpha_i \cdot \rho_i + \alpha_o \cdot \rho_o \tag{7}$$

$\mathbf{F}_e$ in Eq. (2) is the source of the electric stress. It is calculated by taking the divergence of the Maxwell stress in an incompressible flow. The electric stress is given as:

$$\mathbf{F}e = -\frac{1}{2}\mathbf{E} \cdot \mathbf{E}\nabla(\varepsilon_0\varepsilon_r) + q^v\mathbf{E} + \nabla\left(\mathbf{E} \cdot \mathbf{E}\frac{\partial(\varepsilon_0\varepsilon_r)}{\partial\rho}\rho\right) \tag{8}$$

where $\mathbf{E}$ is the electric field strength, ε_0 is the permittivity of vacuum, having a value of $8.854\times10\text{-}^{12}$F/m, ε_r is the relative permittivity of fluid, and q^v is the volume charge density in vicinity of the interface. The first term on the right-hand side of Eq. (8) is the polarization stress, and it acts along normal direction of the interface. Second term of Eq. (8) is the interaction force between electric charges in the electric field acting along the electric field. Last term in Eq. (8) originates from changes in density, and frequently termed as the electro-restriction force density. This term is neglected in incompressible flow.

B. Governing equations for electric field and leaky dielectric model

The electrohydrodynamics in two-phase flows has been reviewed by several researchers.[1,2,45] In electrohydrodynamics, the dynamic current are very small, and the magnetic effects could be ignored. Therefore, the electric field intensity is irrotational ($\nabla\times\boldsymbol{E}$=0). The free charge density is described as:

$$q^v = \nabla \cdot \mathbf{D} = \nabla \cdot (\varepsilon\mathbf{E}) \tag{9}$$

where $\mathbf{D}$ is the electric displacement, ε is constants, and q^v is the volume density of local free charge. Moreover, the charge conservation could be expressed as fellow:

$$\frac{Dq^v}{Dt} = \frac{\partial q^v}{\partial t} + \mathbf{u} \cdot \nabla q^v = -\nabla \cdot (\sigma\mathbf{E}) \tag{10}$$

where $D(\ )/Dt$ is the material derivative, σ is the electric conductivity, and $\boldsymbol{u}$ is the velocity of fluid.

Combining Eq. (9) and (10), the free charge is:

$$\left[\frac{\partial}{\partial t} + \mathbf{u} \cdot \nabla\right]q^v = \frac{Dq^v}{Dt} = -\frac{\sigma}{\varepsilon}q^v = 0 \tag{11}$$

By integration, distribution of the free charge could be obtained as:

$$q^v = q_0^v e^{-\sigma/\varepsilon \cdot t} \tag{12}$$

where q_0^v is the initial free charge density which decays with time. The electric relaxation time $t^E = \varepsilon/\sigma$.

In an electrohydrodynamic flow, viscous time scale of the fluid motion is given as $t^\mu = \rho L^2/\mu$, and L is the fluid characteristic length scale. When fluid is electrically conductive, the electric relaxation time is smaller than the viscous time scale $\left(t^E << t^\mu\right)$; therefore, charge could accumulate at the interface instantaneously as a result of negligible fluid motion and the induced electric field can

reach a steady state. Based on quasi-static assumption, the charge conservation equation (Eq. (9)) is simplified as:

$$\nabla \cdot (\sigma \mathbf{E}) = 0 \tag{13}$$

Due to the absence of an external magnetic field, at small dynamic electrical currents, it is possible to ignore magnetic induction and decouple the electric and magnetic field; therefore, the electric field can be expressed as:

$$\mathbf{E} = -\nabla V \tag{14}$$

where V is the electric potential and the charge conservation equation is:

$$\nabla \cdot (\sigma \nabla V) = 0 \tag{15}$$

For a two-fluid system with constant electrical conductivities, Eq. (12) is reduced to Laplace equations in each medium:

$$\nabla^2 V = 0 \tag{16}$$

Boundary conditions at the interface are given as: continuity of the electric potential and electric current.

$$\|V\| = 0 \text{ and } \|\sigma \nabla V \cdot \mathbf{n}\| = 0 \tag{17}$$

Where$\| \|$ represents a jump across the interface, and $\mathbf{n}$ is the unit normal of the interface.

Electric field strength can be obtained from Eq. (13) and (14), and volume electric density can be obtained from Eq. (10). At quasi-static condition, electric stress only exists at the interface given as:

$$\mathbf{F}e = -\frac{1}{2}\mathbf{E} \cdot \mathbf{E}\nabla(\varepsilon_0 \varepsilon_r) + q^v \mathbf{E} \tag{18}$$

C. Physical model and boundary conditions

A schematic two-dimensional axisymmetric model used in this study is illustrated in Fig. 1. Two identical fluid drops of effective radius R, density ρ_i, viscosity μ_i, relative permittivity ε_i, and electric conductivity σ_i, suspended in another immiscible viscous liquid of density ρ_0, viscosity μ_0, relative permittivity ε_{r0}, and electric conductivity of $\sigma_0$were considered. The computational domain includes the drop phase (represented by subscript i) and the external liquid phase (represented by subscript o). Initially, the two drops were assumed to be identical, spherical, and distance between drops was S. Midpoint between the two drops was at the middle of the parallel-plate capacitor (total distance of $30R$). A steady and uniform electric field (E) was generated along the z direction as electric potential was applied to the two paralleled plates (ϕ_+, ϕ_-). Density of the drops is chosen to be identical to

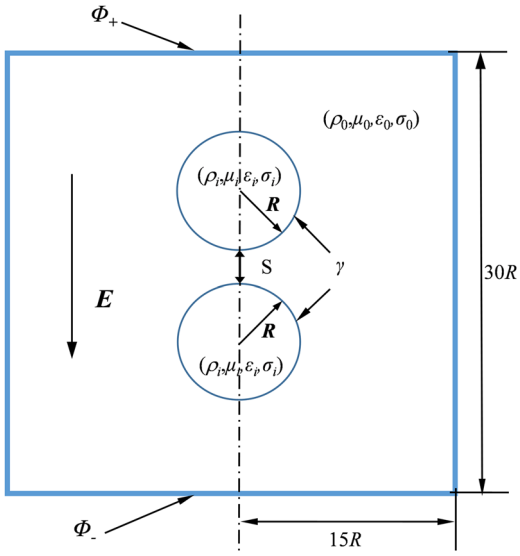

FIG. 1. Schematic of the axisymmetric model of two drops suspended in an immiscible liquid under an external electric field.

TABLE I. Physical properties of the two liquids.

	Density ρ(kg/m^3)	Viscosity μ(kg/m·s)	Permittivity ε_r	Conductivity σ (s/m)	Surface tension γ(N/m)	Permittivity in vacuum ε_0
Corn oil	914	0.0421	3.24	1.06×10^{-11}	1.45×10^{-3}	8.854×10^{-12}
Silicone oil	941	0.0167	2.66	2.67×10^{-12}		

that of the surrounding liquid phase, and therefore, gravitational force can be neglected. A constant interfacial tension coefficient γ was assumed between the two liquids.

Voltages of ϕ_+ and ϕ_- were applied to the upper and lower plates, while a pressure gradient was applied to the right and left edges of the coalescence domain (Fig. 1). At the boundaries, $\partial V/\partial \vec{n} = 0$. Under the effect of electric forces, the drops deform and coalesce. Physical prosperities of the drops and external liquid in present study were listed in Table I. Finite volume method was to discretize the governing equations in the computational scheme. Pressure implicit segmented (PISO) algorithm was employed to capture transient properties of the two phase flow. An iteration step of 10e-5 s was used to fully resolve the drop coalescence process. The electric field was solved by using leaky dielectric model.

D. Validation

Before presenting new numerical results, it is customary to establish the reliability and accuracy of results by benchmarking deformation rates with literature values for experimental and numerical cases. The experimental data by Torza et al,[46] theoretical values,[47] and numerical results by Hua et al,[1] were chosen as basis cases for the validation study. The dispersed fluid drop is 200F silicone oil and continuous liquid is oxidized castor oil. Since the fluids used in this experiment are conductive, the leaky dielectric model is used to simulate the electrical effect. With initial assumption of spherical drop suspending in the stationary liquid, transient simulation is carried out until a steady shape is obtained. In order to characterize the deformation of drop in viscous liquid under electric field, the deformation rate D has been proposed and is calculated using the following expression:

$$D = \frac{L - B}{L + B} \tag{19}$$

where L is the end-to-end length of the droplet measured along the axis of symmetry and B is the maximum breath in the traverse direction.

Fig. 2 shows the comparisons of the present values of deformation rate of dispersed drop in viscous liquid at different an electrical capillary number Ca_E ranging from 0.10 to 0.80. The electrical

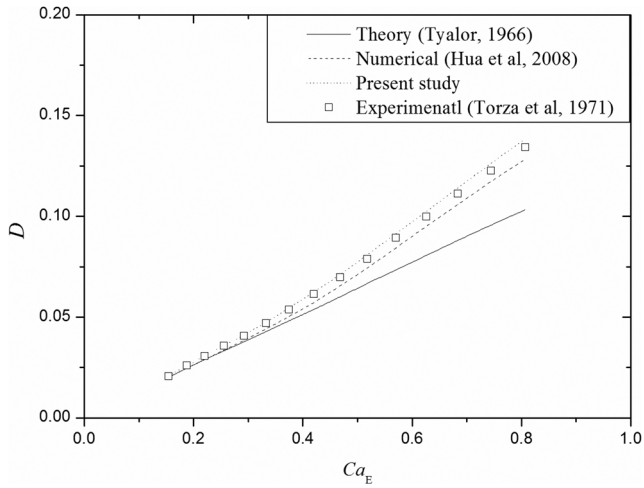

FIG. 2. Model validations.

capillary number is defined as $Ca_E=E^2\varepsilon_0 R/\gamma$ is introduced here to denote the dimensionless strength of the externally applied electric field.[1,2] The drop deformation rate would increase with an increase in electric field strength. The droplet suspended in viscous liquid gradually deforms from sphere to ellipsoid. In present study, the single drop deformation rates are $D = -0.0205$ and $D = -0.063$ under the electrical capillary number of 0.154 and 0.425, while $D = -0.0202$ and $D = -0.062$ in Torza's experimental results. The numerical results in literature were also used to validate the present numerical results, in which the deformation rates of the drop are $D = -0.0203$ and $D = -0.059$. The comparison indicates that present works are good agreement with prior studies. Based on fluid properties (class C, system 16), a comparison of the deformation rate with the Taylor's theory at same conditions are also performed and a good agreement was obtained in slight deformation rate which the value should satisfy $|D|<0.05$.[1,2,47,48] This is because Taylor's theoretical analysis is based on the assumption of small deformation.

III. RESULTS AND DISCUSSION

Two identical-drops of $R = 5.0$mm with initial surface spacing distance of 1.0mm, suspending in viscous stationary liquid under uniform electric field. The corn oil and silicone oils were selected as drop phase and continuous phase respectively. The physical properties of the two fluids are listed in Table I.

A. The mechanism of electro-coalescence

Generally, coalescence could be classified in three stages: 1) drops approaching each other; 2) film thinning/drainage; and 3) film rupture leading to drop-drop coalescence. In an externally applied electric field, electric charge with opposite polarity could be induced on adjacent surfaces of the two drops due to polarization effects. The surface charge density σ_c is illustrated in Fig. 3. Two ends of each drop accumulate electric charges with opposite polarity, which results in the deformation along direction of the electric field. Meanwhile, the two drops separated by a film are brought together due to the electrostatic force between the two spherical drops caused by dipole-dipole interactions. The film is getting thinner as the two drops approaching each other. When film thickness reaches a critical threshold, rupture occurs as a result of tiny disturbance or instability, and the coalescent process starts. Upon contact (of the two drops), a new drop is gradually formed as the surface tension overcomes electric force and the flow resistance. The new formed drop would also be acted upon by polarization forces in an externally applied electric field, as showed in Fig. 3(b), and deforms along direction of the electric field. If the electrostatic force is larger than surface tension, the drop would be continuously stretched and even rupture at sufficient strong electric field strength.

B. Typical behavior of electro-coalescence

Fig. 4 shows the simulated typical coalescence process of two drops under three electric fields of uniform strength. It is clearly shown that the electro-coalescence is highly dependent on electric

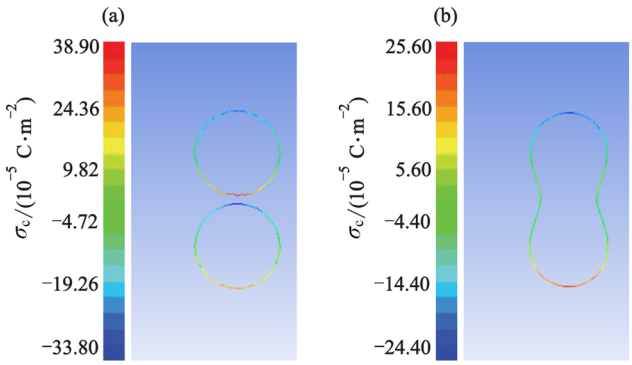

FIG. 3. Charge distributions on the interface.

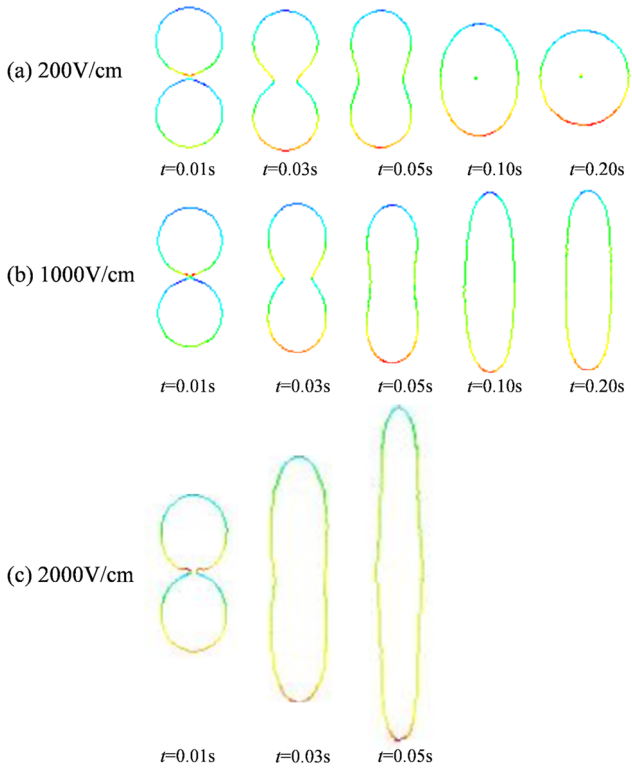

FIG. 4. Three typical drops electro-coalescence processes.

field strength. At low electric field strength (200V/cm), the two drops completed the coalescence into a perfect sphere (Fig. 4(a)), while at large strength (2000V/cm), the two drops coalesced at a faster rate, and the newly formed drop was further stretched and deformed longitudinally till rupture at the two ends (Fig. 4(c)). At the medium electric field strength (1000V/cm), the two drops coalesced and formed a new drop, even though stretched, however stable as a result of the balance between surface tension and the electrostatic force (Fig. 4(b)). The numerical results (Fig. 4) indicated that deformation rate increases with the applied electric field strength, while the full electro-coalescence rate decreases. A plenty of works about electro-coalescence indicated that there is critical threshold of the electric field strength is present that, above which, the two drops would rupture and separate after coalesce. Below the threshold, the two drops complete the coalescence and reach a stable state. Deformation could occur to the newly formed drop relating to the applied electric strength. The surface charge density induced by the polarization effects could enhance drop coalescence and induce further deformation. When the applied electric field strength was above a critical value (e.g. at 2000V/cm), the two drops were firstly attracted to and contacted each other. Then the new drop was deformed and elongated beyond a critical length that, the surface tension could no longer balance the electrostatic stretching force, and coalescence failed. As the electric field strength further increased, it was possible that the individual drop would deform longitudinally, and rupture at end of the drop could occur before they made the contact. This is due to a significant larger electrostatic force than surface tension and fluid resistance forces. Meanwhile, according to published literature, the onset of drop break-up occurs could be estimated by an electric Weber number ($We_E=\varepsilon E^2 R_{eq}/\gamma$). At the electric field strength of E = 2000V/cm, the corresponding We_E number is obviously larger than the critical number provided by some previous research work.[49]

C. Surface morphology of coalescence

In the present study, electro-coalescence of the identical drops was numerically simulated. Radius of the drop was R and shortest distance between drop surfaces was set to S, as showed in Fig. 1. Four

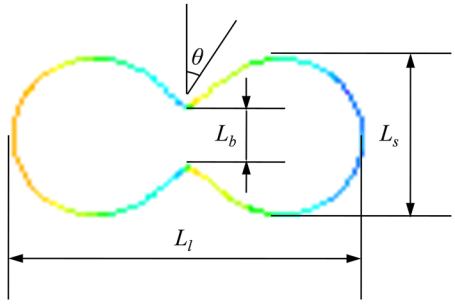

FIG. 5. Surface morphology of drop during electro-coalescence process.

electric field strengths were applied to the system. Morphologies of the drops during coalescence were captured and analyzed. Fig. 5 shows the representative characteristic lengths of the meniscus liquid bridge (L_b), minor axis (L_s), major axis (L_l), and cone angle (θ). Measurements were made at least three times and an averaged value was taken under each operating condition. Non-dimensionalized characteristic lengths could be obtained as the ratios to meniscus liquid bridge ($D_b = L_b/2R$), minor axis ($D_s = L_s/2R$), and length major axis ($D_l = L_l/(S+4R)$), respectively. Because the electric field strength of E = 2000 V/cm is apparently larger than critical threshold, the coalesced prolate droplet would be elongated by electric force to be a critical length and finally break up. So the characteristic sizes of the coalesced droplet before disintegration (about t =1.5s) were calculated. Meanwhile, the total length of coalesced droplet L_l is much larger than the radius of drop R, and the width of coalesced droplet L_s is much smaller than radius of drop R within a period of 0.5s. So we only calculated the values of L_l and L_s before t = 0.5s.

For the typical evolution of interfacial shape between the two identical drops during coalescence (Fig. 4), length ratio of the meniscus liquid bridge (D_b) overtime was displayed in Fig. 6. Four external field strengths were considered. It was observed that, the length ratio of meniscus bridge (D_b) could be always increasing, firstly increasing then being constant or firstly increasing and then decreasing. At lower electric field strength (200V/cm and 500V/cm), radius of the liquid bridge constantly increased until a cylindrical shape was formed. Following that, the two drops untied and merged into an ellipse close to the shape of a circle. Length ratio of the meniscus liquid bridge could reach the equilibrium state following a steady increase. Ata medium electric field strength of 1000V/cm, length ratio of the meniscus liquid bridge also steadily increased and reached a constant value. Compared to the lower electric field strength, radius of the cylinder formed by liquid bridge was smaller. On the other hand, coalescence at the medium electric field strength took less time of 0-0.6s versus 0-1.5s at the lower

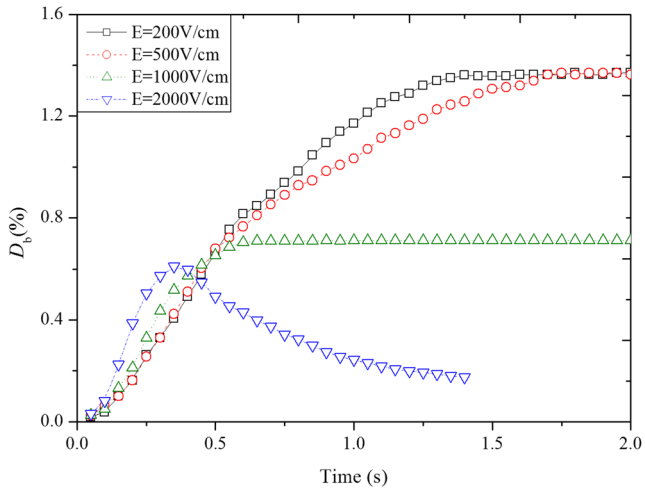

FIG. 6. Comparison of length ratio of the meniscus liquid bridge.

strength. Beyond the critical field strength where coalescence failed, length ratio of the meniscus liquid bridge increased sharply between 0-0.4s and then it decreased from 0.4 to 1.2s.

Fig. 6 clearly indicated that length ratio of meniscus bridge (D_b) was affected by the electric field strength. Rate of change of the meniscus bridge length ratio increased with an increase in the applied electric field strength. This was due to: 1) the increased accumulation of opposite charges on surface of the adjacent drops; and 2) larger electrostatic forces caused by dipole-dipole interaction. Speed of the coalescence was clearly enhanced with an increase in the electric field strength (below the critical value). At low electric field strengths (200V/cm and 500V/cm), the two drops fully coalesce and formed a new elliptic drop close to circular shape. Other electric field strengths were shown to induce coalesces of the two drops and form elongated shapes. It was concluded that, low electric field strength induced favorable coalescence process, though it took more time to complete the process.

The simulated evolution of the length ratio (D_l) of major axis was shown in Fig. 7. Typical coalescence processes could be observed from the figure. At low electric field strengths (200V/cm and 500V/cm), the length ratio of major axis was relative stable initially, and then it was gradually decreasing, and eventually reached a steady state. During this process, the two drops made contact in a very short period duration (0-0.6s). The counter ends of the two adjacent drops have no time to respond and therefore kept the original length. At the time interval of 0.7-1.5s, the two drops started coalescing and the major axis became shorter under the influence of the surface tension. Union of the two drops would reach to an equilibrium state with ellipsoidal shape that bridge between the two drops was cylindrical and no longer change. At medium electric field strength (1000V/cm), length ratio of the major axis firstly increased (0-0.9s), and then reached a stable state (>1.0s) (Fig. 7). During this time, the two drops started coalesce. Compared with that of the lower electric field strength, union of the two drops was more elongated. Eventually, union of the two drops reached an equilibrium state and became elliptic. At higher electric field strength (2000V/cm) beyond the critical value, length ratio of the major axis constantly increased until the two drops or the union suddenly stretched and broke up.

For drops succeeded to coalesce, length ratio of the major axis experienced two stages: increasing\decreasing stage and stable stage. Each stage was a manifest of the balance between electrostatic force and the surface tension force. At lower electric field strengths (200 V/cm and 500V/cm)), the electrostatic force is smaller than the surface tension, and surface tension dominated coalescence process. Length of the major axis gradually shrank until an equilibrium state was reached. At medium electric field strength (1000V/cm), the electrostatic force dominated coalescence process, and length of the major axis gradually elongated until the equilibrium state was reached. For both cases, after reaching the equilibrium state, major axis of the united drops would no longer change.

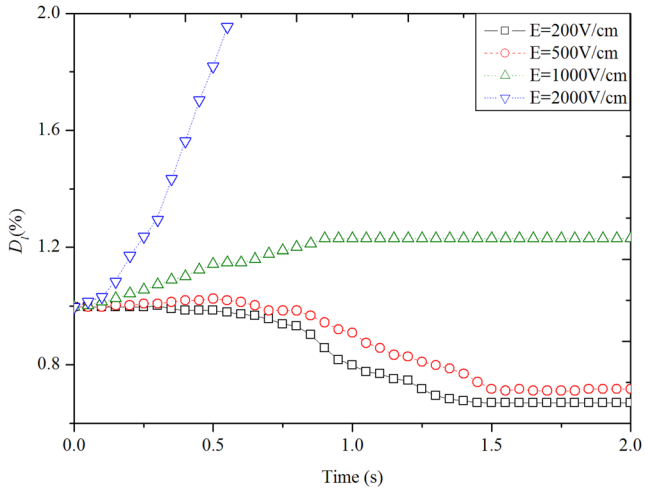

FIG. 7. Comparison of length ratio of major axis.

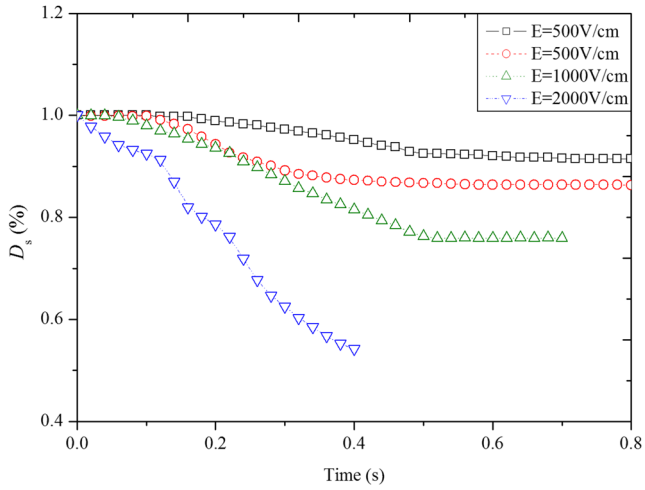

FIG. 8. Comparison of length ratio of minor axis.

At higher electric field strength (2000V/cm), drops approached, contacted and deformed along the direction of electric field rapidly, until elongation led to final rupture as a result of the surface tension could no longer balance the electrostatic force.

Simulated evolution of length ratio (D_s) for minor axis was presented in Fig. 8. Definition of the minor axis and cone angle was illustrated in Fig. 5. Minor axis was present when cone angle was less than 90°. It was clearly shown that, during successful coalesce, length ratio of the minor axis firstly decreased and reached a steady state. During failed coalesce, length ratio of the minor axis steadily decreased until drop rupture occurred. Decreasing rate of the length ratio for minor axis was shown to increase with applied electric field strength as electrostatic force was direct proportional to the applied value. Among the three electric field strengths under which coalesce succeeded, equilibrium state was more easily obtained at electric strength of 500V/cm because it took the least effort to obtain a balance between the electrostatic force and surface tension. This could be considered as favorable electric field strength to the coalescence process.

When the drops approached to each other, leading edges of the drops would be elongated. Elongation induced drop contact and coalesce process started. The cone angle of drop contacting was defined in Fig. 5 as the angle formed by the tangential of the drop and the central symmetric axis line. The cone angle variation evolution was illustrated in Fig. 9. At low electric field strengths

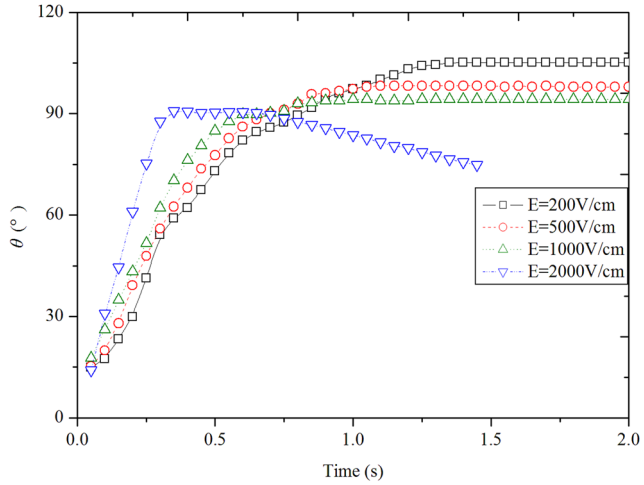

FIG. 9. Comparison of cone angle.

(200V/cm and 500V/cm), cone angle was steadily increased to 90°. A 90° cone angle indicated that the meniscus bridge between drops became cylindrical. Cone angle would continue to increase as the surface tension was still larger than electrostatic force. A steady cone angle was attained until a balance was achieved between the surface tension and electrostatic force. At the medium electric field strength (1000V/cm), cone angle steadily increased until a stable value was reached (<90°). At this stage, Meniscus Bridge between the two drops became cylindrical and surface tension neutralized the electrostatic force. Union of the two drops eventually transformed into an ellipse, and cone angle could be either larger or smaller than 90°. At very large electrical field strength (>critical value) cone angle firstly increased to a maximum value. Then it steadily decreased as the electrostatic force was larger than the surface tension. At breaking point, rupture of the drops occurred at the two ends; therefore, cone angle was not immediately affected. It was concluded that variation of cone angle development could be used to classify the drop coalescence process.

IV. CONCLUSIONS

Coalescence model (VOF method and leaky dielectric model) under uniform electric field was employed to study the coalescence behavior of drop pair in viscous liquid. The behavior of meniscus liquid bridge, major axis, minor axis and cone angle were analyzed under different electric field strengths. For successful coalescence of drops, the length of meniscus liquid bridge, major and minor axis would get a constant value, while the cone angle also would obtain a value of 90°. For failed coalescence of drops, all the length of meniscus liquid bridge, major and minor axis, and cone angle could not obtain a constant value. The results indicated that electric field strength significantly affected coalescence of identical drop pair in viscous the liquid, and there exists a critical value, below which the successful coalescence of drop pair could be finished. Typical coalescence processes could be observed in the simulation and union of the drops could lead to sphere or elongated ellipsoid. The presented numerical results are interesting and significant in fundamental study on electro-coalescence, which could provide useful data for further theoretical study and numerical simulation. An excellent outcome may be achieved with considering larger number of parameters. Therefore, more studies are necessary either experimentally or theoretically to enhance the understanding of this phenomenon.

ACKNOWLEDGMENTS

The authors would like to acknowledge the research grant from National Natural Science Foundation of China (No. 51106064, No. 51704126), Natural Science Foundation of Jiangsu Province, China (No. BK20171301, BK20170551, and BK20150511), China Postdoctoral Science Foundation (2018M632245), a project funded by the Priority Academic Program Development of Jiangsu Higher Education Institutions (PAPD) and a project supported by Jiangsu University for NSFC (FCJJ2015001).

[1] J. Hua, K. L. Liang, and C. H. Wang, "Numerical simulation of deformation/motion of a drop suspended in viscous liquids under influence of steady electric fields," Phys. Fluids **20**, 113302 (2008).
[2] Z. Wang, Q. Dong, Y. Zhang, J. Wang, and J. Wen, "Numerical study on deformation and interior flow of a droplet suspended in viscous liquid under steady electric fields," Adv. Mech. Eng. **6**, 532797 (2014).
[3] Y. Wang and P. Ming, "Effect of radius ratios of two droplets on coalescence-induced self-propelled jumping," AIP Adv. **8**, 065320 (2018).
[4] C. Guo and L. He, "Coalescence behavior of two large water-drops in viscous oil under a DC electric field," J. Electrostat. **72**(6), 470 (2014).
[5] J. S. Eow, M. Ghadiri, A. O. Sharif, and T. J. Williams, "Electrostatic enhancement of coalescence of water droplets in oil: A review of the current understanding," Chem. Eng. J. **84**, 173 (2001).
[6] C. T. Chen, J. R. Maa, Y. M. Yang, and C. H. Chang, "Effects of electrolytes and polarity of organic liquids on the coalescence of droplets at aqueous-organic interfaces," Surf. Sci. **406**(1-3), 167 (1998).
[7] D. Sun, S. C. Jong, X. D. Duan, and D. Zhou, "Demulsification of water-in-oil emulsion by wetting coalescence materials in stirred- and packed-columns," Colloid Surface A **150**(1-3), 69 (1999).
[8] C. A. R. Pearce, "The mechanism of the resolution of water-in-oil emulsions by electrical treatment," Br. J. Appl. Phys. **5**(4), 136 (1954).
[9] S. E. Taylor, "Investigations into the electrical and coalescence behavior of water-in-crude oil emulsions in high voltage gradients," Colloid Surface **29**(1), 29 (1988).

[10] P. J. Bailes and E. H. Stitt, "Column liquid contacting with vigorous agitation balanced by electrostatic coalescence," Chem. Eng. Res. Des. **65**, 514 (1987).
[11] J. S. Eow and M. Ghadiri, "Electrostatic enhancement of coalescence of water droplets in oil: A review of the technology," Chem. Eng. J. **85**(2-3), 357 (2002).
[12] H. A. Pohl, "Some effects of nonuniform fields on dielectrics," J. Appl. Phys. **29**(8), 1182 (1958).
[13] L. C. Waterman, "Electrical coalescers," Chem. Eng. Prog. **61**(10), 51 (1965).
[14] M. Mohammadi, S. Shahhosseini, and M. Bayat, "Electrocoalescence of binary water droplets falling in oil: Experimental study," Chem. Eng. Res. Des. **92**, 2694 (2014).
[15] P. J. Bailes and S. K. L. Larkai, "Influence of phase ratio on electrostatic coalescence of water-in-oil dispersions," Chem. Eng. Res. Des. **62**, 33 (1984).
[16] T. Hano, T. Ohtake, and K. Takagi, "Demulsification kinetics of W/O emulsion in an A.C. electric field," J. Chem. Eng. Jpn. **21**(4), 345 (1988).
[17] S. S. Wang, C. J. Lee, and C. C. Chan, "Demulsification of water-in-oil emulsions by use of a high voltage AC field," Sep. Sci. Technol. **29**(2), 159 (1994).
[18] S. E. Taylor, "Theory and practice of electrically-enhanced phase separation of water-in-oil emulsions," Chem. Eng. Res. Des. **74**(5), 526 (1996).
[19] Y. Zhang, Y. Liu, and R. Ji, "Dehydration efficiency of high-frequency pulsed DC electrical fields on water-in-oil emulsion," Colloid Surface A **373**(1-3), 130 (2011).
[20] Y. Zhang, Y. Liu, R. Ji, B. Cai, H. Li, and F. Wang, "Dehydration efficiency of water-in-model oil emulsions in high frequency pulsed dc electrical field: Effect of physical and chemical properties of the emulsions," J. Disper. Sci. Technol. **33**(11), 1574 (2012).
[21] S. H. Mousavi, M. Ghadiri, and M. Buckley, "Electro-coalescence of water drops in oils under pulsatile electric fields," Chem. Eng. Sci. **120**, 130 (2014).
[22] S. Mhatre, S. Deshmukh, and R. M. Thaokar, "Electrocoalescence of a drop pair," Phys. Fluids **27**, 092106 (2015).
[23] H. Morteza, "Coalescence behaviour of water droplets in water-oil interface under pulsatile electric fields," Chinese J. Chem. Eng. **24**(9), 1147 (2016).
[24] V. Vivacqua, S. Mhatre, M. Ghadiri, A. M. Abdullah, A. Hassanpour, M. J. Al-marri, B. Azzopardi, B. Hewakandamby, and B. Kermani, "Electrocoalescence of water drop trains in oil under constant and pulsatile electric fields," Chem. Eng. Res. Des. **104**, 658 (2015).
[25] J. S. Eow and M. Ghadiri, "Drop–drop coalescence in an electric field: The effects of applied electric field and electrode geometry," Colloid Surface A **219**(1-3), 253 (2003).
[26] T. J. Williams and A. G. Bailey, "Changes in the size distribution of a water-in-oil emulsion due to electric field induced coalescence," IEEE T. Ind. Appl. **IA-22**(3), 536 (1986).
[27] P. Atten, "Electro-coalescence of water droplets in an insulating liquid," J. Electrostat. **30**, 259 (1993).
[28] J. S. Eow, M. Ghadiri, and A. O. Sharif, "Electro-hydrodynamic separation of aqueous drops from flowing viscous oil," J. Petrol. Sci. Eng. **55**(1-2), 146 (2007).
[29] M. Chiesa, S. Ingebrigtsen, J. A. Melheim, P. V. Hemmingsen, E. B. Hansen, and Ø. Hestad, "Investigation of the role of viscosity on electrocoalescence of water droplets in oil," Sep. Purif. Technol. **50**(2), 267 (2006).
[30] H. Aryafar and H. P. Kavehpour, "Electrocoalescence: Effects of DC electric fields on coalescence of drops at planar interfaces," Langmuir **25**(21), 12460 (2009).
[31] R. S. Allan and S. G. Mason, "Effects of electric fields on coalescence in liquid-liquid systems," Trans. Faraday Soc. **57**, 2027 (1961).
[32] T. Hirato, K. Koyama, T. Tanaka, Y. Awakura, and H. Majima, "Demulsification of water-in-oil emulsion by an electrostatic coalescence method," Mater. Trans. **32**(3), 257 (1991).
[33] I. G. Harpur, N. J. Wayth, A. G. Bailey, M. T. Thew, T. J. Williams, and O. Urdahl, "Destabilisation of water-in-oil emulsions under the influence of an A.C. electric field: Experimental assessment of performance," J. Electrost. **40-41**, 135 (1997).
[34] M. Mohammadi, S. Shahhosseini, and M. Bayat, "Direct numerical simulation of water droplet coalescence in the oil," Int. J. Heat Fluid Fl. **36**(8), 58 (2012).
[35] M. Mohammadi, S. Shahhosseini, and M. Bayat, "Numerical study of the collision and coalescence of water droplets in an electric field," Chem. Eng. Technol. **37**(1), 27 (2014).
[36] M. Mohammadi, "Numerical and experimental study on electric field driven coalescence of binary falling droplets in oil," Sep. Purif. Technol. **176**, 262 (2017).
[37] V. Vivacqua, S. Mhatre, M. Ghadiri, A. M. Abdullah, A. Hassanpour, M. J. Al-marri, B. Azzopardi, B. Hewakandamby, and B. Kermani, "Analysis of partial electrocoalescence by level-set and finite element methods," Chem. Eng. Res. Des. **114**, 180 (2016).
[38] B. Sakakibara and T. Inamuro, "Lattice Boltzmann simulation of collision dynamics of two unequal-size droplets," Int. J. Heat Mass Tran. **51**(11-12), 3207 (2008).
[39] Y. Shi, G. J. Tang, and H. H. Xia, "Investigation of coalescence-induced droplet jumping on super hydrophobic surfaces and liquid condensate adhesion on slit and plain fins," Int. J. Heat Mass Tran. **88**, 445 (2015).
[40] Y. Meleán and L. D. G. Sigalotti, "Coalescence of colliding van der Waals liquid drops," Int. J. Heat Mass Tran **48**(19-20), 4041 (2005).
[41] B. B. Wang, X. D. Wang, T. H. Wang, G. Lu, and W. M. Yan, "Electro-coalescence of two charged droplets under constant and pulsed DC electric fields," Int. J. Heat Mass Tran. **98**, 10 (2016).
[42] S. W. Choi, D. E. Lee, W. I. Lee, and H. S. Kim, "Analysis of coalescence behavior for compressed droplets," Appl. Surf. Sci. **397**, 57 (2017).
[43] M. N. Reddy and A. Esmaeeli, "The EHD-driven fluid flow and deformation of a liquid jet by a transverse electric field," Int. J. Multiphase Flow **35**(11), 1051 (2009).

[44] J. U. Brackbill, D. B. Kothe, and C. A. Zemach, "A continuum method for modeling surface tension," J. Comput. Phys. **100**, 335 (1992).
[45] D. A. Saville, "Electrohydrodynamics: The Taylor-Meelcher leaky dielectric model," Annu. Rev. Fluid Mech. **29**, 27 (1997).
[46] S. Torza, R. G. Cox, and S. G. Mason, "Electrohydrodynamic deformation and burst of liquid drops," Philos. T. R. Soc. B **269**(1198), 295 (1971).
[47] G. Taylor, "Study in electrohydrodynamics I: The circulation produced in a drop by electrical field," P. Roy. Soc. A-Math. Phy. **291**(1425), 159 (1966).
[48] J. R. Melcher and G. I. Taylor, "Electrohydrodynamics: A review of the role of interfacial shear stresses," Annu. Rev. Fluid Mech. **1**, 111 (1969).
[49] J. S. Eow, M. Ghadiri, and A. Sharif, "Deformation and breakup of aqueous drops in dielectric liquids in high electric fields," J. Electrostat. **51-52**, 463 (2001).